Lab on a Chip

Cite this: *Lab Chip*, 2012, **12**, 5142–5145

www.rsc.org/loc

TECHNICAL INNOVATION

Centrifugo-dynamic inward pumping of liquids on a centrifugal microfluidic platform†

Steffen Zehnle,*[a] Frank Schwemmer,[b] Günter Roth,[abc] Felix von Stetten,[ab] Roland Zengerle[abc] and Nils Paust[a]

Received 17th August 2012, Accepted 3rd October 2012
DOI: 10.1039/c2lc40942a

We present a method to pump liquids in a centrifugal microfluidic spinning disk from a radial outward position to a radial inward position. Centrifugal forces are applied to compress air in a cavity, this way storing pneumatic energy. The cavity is connected to an outlet channel having a lower hydraulic resistance compared to the inlet channel. The stored pneumatic energy is quickly released by fast reduction of rotational frequency. This way liquid is transported mainly through the channel with lower resistance, directing the liquid radially inwards. Pump efficiencies of >75% per pump cycle have been demonstrated for water, ethanol, a highly viscous lysis buffer and whole blood. By employing three pump cycles, water has been pumped radially inwards with an efficiency of >90%. The inward pumping requires centrifugation only, which is intrinsically available on every centrifugal microfluidic platform.

Introduction

The last decade has witnessed significant advances in centrifugal microfluidics (MF). The MF chips in compact disk format have been fabricated and used for automated biological assays.[1–3] Centrifugal forces are employed to propel liquid reagents and samples through the MF channels into processing chambers, where various unit operations have been successfully realized. These include mixing, sedimentation, separation, valving, metering and aliquoting.[2,4–12] The developed centrifugal MF disks are cost-effective and disposable; enable parallel processing; and can be used in standard processing devices, such as laboratory centrifuges, DVD drives and thermocyclers.[13–15]

Inherently, centrifugal forces propel liquids radially outwards, only, which is considered a major limitation of centrifugal platforms, as the radial path provided is limited by the radius of the centrifugal disks. Long fluidic paths can be realized by circumferential spiraled channels.[16] However, many functional building blocks of analysis, such as cell lysis from bacteria,[17] DNA extraction from whole blood[10] and genotyping of purified DNA samples[18] consume the entire radial disk path. Therefore, the development of complete sample-to-answer systems would heavily profit from a method to pump liquids back towards the center of rotation, *e.g.* to enable a coupling of sample preparation with downstream genotyping. Similarly, there is a limitation of space in the case of liquid reagent pre-storage based LabDisk assays, where all the liquids have to be stored and released close to the center of rotation. Therefore, the pumping of liquids radially inwards will provide the freedom to store liquids at any position on the disk, which will be highly useful to enable the implementation of complex biological assays.

The existing state-of-the-art approaches employ assistive means to pump liquids radially inwards. An infrared radiation source has been used to thermally expand an air bubble that displaces liquid radially inwards.[19] Similarly, other approaches have used pressurized air from an external gas container[20,21] or an additional displacer liquid[22] to move the sample liquid towards the center of rotation. The methods using capillary and pneumatic forces for reciprocating the flow in an MF disk do not enable inward pumping, because the liquids finally cannot escape from the single channel in which they are moved back and forth.[5,23]

In contrast to the state-of-the-art we introduce a method to pump liquids radially inwards, employing centrifugation only. This unit operation has been demonstrated in a fluidic test module that has been fully optimized and characterized. The optimization of parameters is done in a network simulation which has been employed as a tool to predict the fluidic characteristics in centrifugal platforms.

Functional principle

The centrifugo-dynamic inward pumping (CDIP) has been realized in a MF process that employs pneumatic pumping. The basic principle of pneumatic pumping has been presented recently for mixing by reciprocating flow and siphon valving.[5,9,24]

[a]*HSG-IMIT – Institut für Mikro- und Informationstechnik, Georges-Koehler-Allee 103, 79110 Freiburg, Germany. E-mail: steffen.zehnle@hsg-imit.de*
[b]*Laboratory for MEMS Applications, IMTEK - Department of Microsystems Engineering, University of Freiburg, Georges-Koehler-Allee 103, 79110 Freiburg, Germany*
[c]*BIOSS – Centre for Biological Signalling Studies, University of Freiburg, 79110 Freiburg, Germany*
† Electronic supplementary information (ESI) available: Network model, results from simulation and strobed experimental videos of centrifugo-dynamic inward pumping. See DOI: 10.1039/c2lc40942a

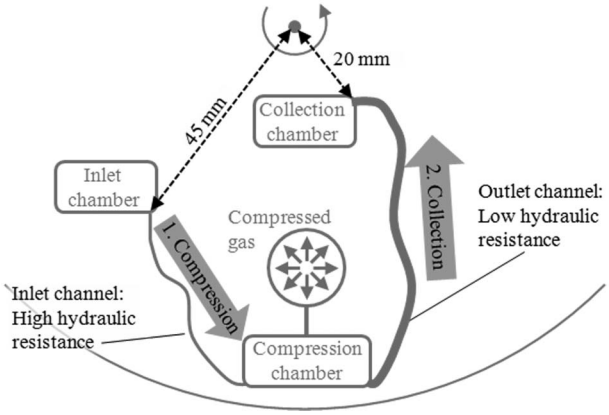

Fig. 1 Functional principle of centrifugo-dynamic inward pumping (CDIP) in a centrifugal microfluidic (MF) disk.

We have taken into account the viscous dissipation of fluids in microchannels and used the energy of a compressed gas bubble for passive inward pumping, as illustrated in Fig. 1 and 2. The pumping action is accomplished in two phases:

1. Compression: By centrifugation at high rotational frequency, the sample liquid is pumped by centrifugal forces from the inlet chamber through a narrow inlet channel into a radially outer compression chamber. The air in the compression chamber is encapsulated and compressed by the centrifugal pressure of the sample liquid in the inlet and outlet channels. This converts the centrifugal potential energy of the sample liquid into the potential energy of the pressurized air bubble. Subsequently, when the fill levels in the inlet channel, the compression chamber and the outlet channel reach equilibrium, the centrifugal pressure counterbalances the overpressure of the encapsulated air bubble in the compression chamber.

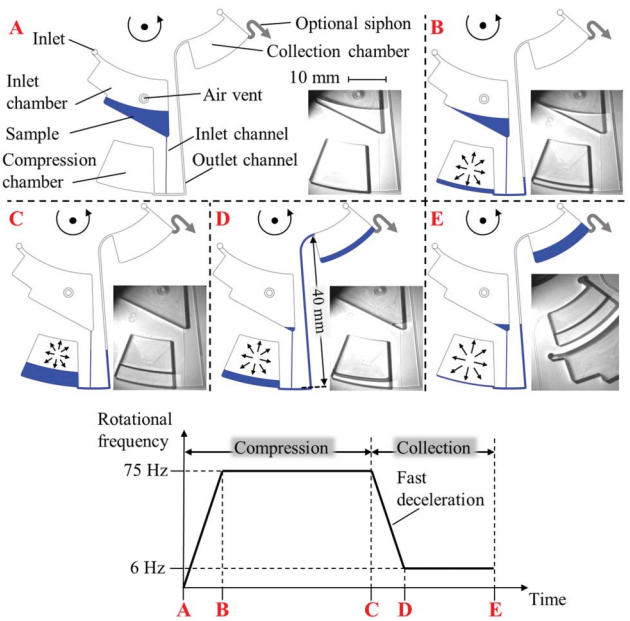

Fig. 2 Implementation of CDIP in a centrifugal MF disk: **A:** The sample liquid is pipetted into the inlet chamber. **B:** At high rotational speed, the liquid is loaded into the compression chamber and compresses a gas volume. **C:** Gas overpressure in the compression chamber is balanced by centrifugal pressure in the channels. **D:** Fast deceleration of the disk rapidly reduces centrifugal pressure, so that the compressed gas volume quickly expands and displaces the liquid mainly through the outlet channel. **E:** The liquid stream in the outlet channel tears off, thereby terminating the pumping process. An optional siphon can be used to route the liquid again radially outwards, provided that the fill level in the collection chamber exceeds the siphon crest.

2. Collection: The fast deceleration of the MF disk to lower rotational frequencies rapidly decreases the centrifugal forces and hence the centrifugal pressure of the liquid exerted on the encapsulated air volume. The relative overpressure of the air leads to fast expansion of the air volume, by which the majority of the sample liquid is displaced through an outlet channel of large cross-section and low hydraulic resistance. At the same time, a minor fraction of the sample liquid is displaced through the inlet channel which has a smaller cross-section and higher hydraulic resistance. The high viscous dissipation in the narrow inlet channel that counteracts the bubble overpressure limits the backflow of liquid into the inlet chamber. This enables the major part of the sample liquid to be transferred to the radially inner collection chamber for further liquid processing. Such a passive pumping process is possible only by employing a dynamic method that involves a rapid "switch-off" of centrifugal pressure.

Modeling and simulation

A high hydraulic resistance in the inlet channel in comparison to the outlet channel ($R_{hyd,in} \gg R_{hyd,out}$) is essential for CDIP.

However, the pumping process still needs to be optimized in order to maximize the pump efficiency, which is defined as

$$\eta = \frac{V_{pumped}}{V_{total}}$$

where V_{pumped} is the volume of the sample liquid collected in the collection chamber after pumping, while V_{total} is the total initial sample volume. We developed a network model to compute the pump efficiency for specific geometries and specific spin frequency protocols. The MF structure was broken down into single lumped model elements for all chambers and channels that have either radial or circumferential orientation. According to Kirchhoff's law applied to MF circuit theory, the pressure differences in a closed loop of fluidic elements sum up to zero.[25] The pressure difference, Δp, across each fluidic element is determined by the sum of the radial centrifugal pressure p_c, the viscous pressure drop p_v, the circumferential Euler pressure p_E, the inertial pressure p_i and the capillary pressure p_{cap}:

$$\Delta p = p_c + p_v + p_E + p_i + p_{cap}$$

The various types of pressures are described below,

$$p_c = \frac{1}{2}\rho\omega^2\left(r_2^2 - r_1^2\right) \quad p_v = -28.4\,\mu L\frac{1}{a^4}q$$

$$p_E = \rho L\dot{\omega}r \quad p_i = -\frac{\rho L}{A}\dot{q} \quad p_{cap} = \frac{4\sigma\cos\theta}{a}$$

where ρ represents the liquid density; ω is the angular spin frequency; r_1 and r_2 are the minimum and maximum radial positions of the liquid, respectively; μ is the liquid viscosity; L is the path length occupied by liquid; A is the cross-sectional area; a is the edge length

of the cross-sectional area in channels; q is the volumetric flow rate; r is the mean radial position of circumferential channels; σ is the surface tension; and θ is the contact angle. The encapsulated air volume was considered as an ideal gas for the developed model which is specified further in the ESI.†

The experimental pumping structure employs an inlet channel with a cross-sectional area of 120 μm × 120 μm. A network simulation setup in Saber 2004.06 (Synopsys, CA, USA) was used to optimize the outlet channel diameter in order to get the maximum pump efficiency, η. For 100–300 μl water samples, η reaches its maximum when the cross-sectional area of the outlet channel is 450 μm × 450 μm. For smaller diameters, $R_{hyd,out}$ approaches $R_{hyd,in}$ which makes the pumping mechanism ineffective. Larger diameters lead to losses as the increased amount of liquid does not reach the collection chamber because it remains in the outlet channel as dead volume.

Fabrication

The MF disk (Ø = 130 mm) was designed in SolidWorks 2011 (Concord, MA, USA) and manufactured in-house by HSG-IMIT Lab-on-a-Chip Design and Foundry Service (www.loac-hsg-imit.de/en/design-foundry-service). In brief, the channels were milled into 4 mm thick PMMA disks (Plexiglas, Evoniks, Germany) *via* CNC micromilling. The disks were sealed with a pressure sensitive adhesive polyolefin foil (#900320, HJ Bioanalytik, Germany) using a laminator roll. This allowed for the reuse of disks as the adhesive foil can be removed manually after each experiment. As ethanol dissolves the adhesive causing the foil to delaminate from the disk, thermally-bonded disks were employed for the ethanol samples. The thermally-bonded disks were made by sealing the PMMA disks with 50 μm thick polystyrene (PS) foils (ErgoWin, Norflex, Germany) at 105 °C for 10 min under a force of 4 kN that was generated by a custom built hot press (Wickert, Germany).

Experiments

The disk was mounted onto an EC motor (Maxon, Switzerland) which was synchronized to an optical setup that records one image per revolution. The CDIP was tested by employing typical biologically-relevant liquid reagents having varying densities, viscosities and surface tensions. These include deionized water, ethanol, whole blood and a commercial lysis buffer (*Buffer AL* procured from Qiagen, Germany; a highly viscous lysis buffer used in the DNA extraction from whole blood) (Table 1). The high viscosity of the lysis buffer results from detergents and a high concentration of chaotropic salts. It was measured with the rheometer Physica MCR 101 (Anton Paar, Germany).

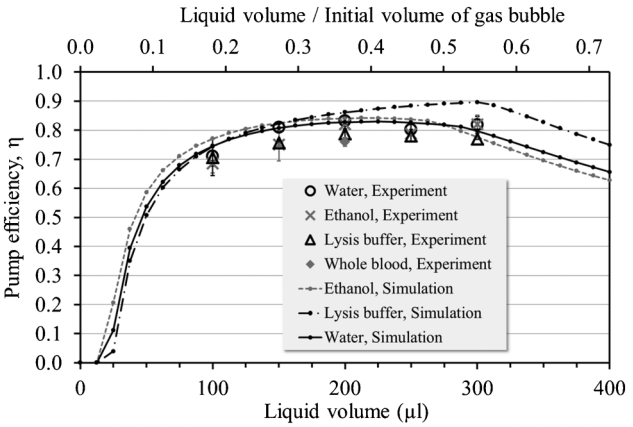

Fig. 3 CDIP of liquids with varying volumes at a deceleration of 30 Hz s^{-1}. The pump efficiency reaches its maximum between 200–300 μl.

Fig. 2 shows the implementation of the inward pumping module in the centrifugal MF disk. The sample liquids were pipetted into the inlet chamber through an inlet port. In order to investigate the volume dependence of the pump efficiency, the sample volumes were varied between 100–300 μl. The deceleration was varied between 1–30 Hz s^{-1} to study the change in pump efficiency with the deceleration. In the case of whole blood, a 200 μl sample (hematocrit: 42%, which is in the physiological range of 37–52%) was applied at 10 Hz s^{-1} and 30 Hz s^{-1}. All experiments were carried out in triplicates. The optional siphon enables the routing of liquid for further downstream processing after the termination of the inward pumping.

Results and discussion

The recorded real-time images were used to measure the fill levels in the collection chamber employing Photoshop CS4 (Adobe Systems Incorporated, CA, USA). These fill levels were applied in the SolidWorks construction to determine the pumped volume. The resulting pump efficiency, η, was plotted against the total liquid volume that was applied (Fig. 3). The simulation demonstrates the need for a minimum liquid volume to achieve $\eta > 0$, which is due to the dead volume taken up by the channels. Our experiments demonstrate pump efficiencies of more than 75% for sample volumes between 200–300 μl. However, the simulation shows a decrease in the pump efficiency above a certain sample volume as the compression chamber has limited sample capacity. The experimental pump efficiency of the lysis buffer is lower than the simulated one, which is due to pinning effects in the compression chamber during collection.

Table 1 The properties of sample liquids used for the characterization of CDIP

	Density (g cm^{-3})	Viscosity (mPa s)	Surface tension (mN m^{-1})
Water	1.00	1.00	72.9
Ethanol	0.79	1.20	23.0
Lysis buffer	1.16	16.0	N/A
Whole blood	~1.06[a]	~4–9[a]	~60[a]

[a] The properties of blood change during centrifugation due to sedimentation of the cells. The viscosity is shear-rate dependent.

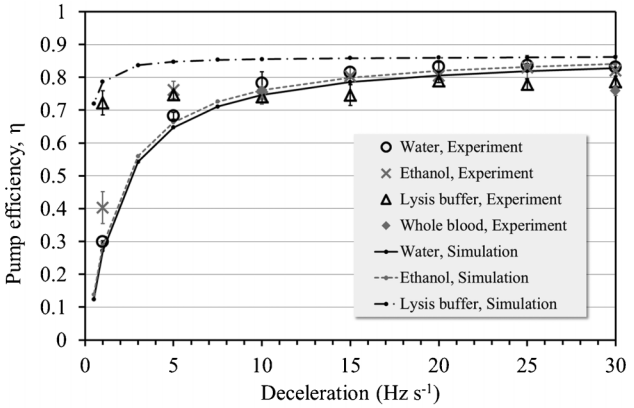

Fig. 4 CDIP of 200 µl liquid samples at varying decelerations. The pump efficiency rises with the increasing deceleration.

The fast deceleration (Fig. 4) of the MF disk is of paramount importance to achieve high pump efficiencies. Otherwise, the hydrodynamic effects during collection get ineffective, which leads to the pumping of the sample liquid back into the inlet chamber. The increased pump efficiency of ethanol at low deceleration is attributed to the increased hydraulic resistance of the inlet channel, which is a result of the fabrication process of the disks for ethanol processing: The high temperatures and pressures during thermal bonding of PS on PMMA induce shrinkage of the MF channels, resulting in a decrease of 12% in the cross-sectional area.

It was demonstrated that also whole blood can be pumped inwards with a pump efficiency of more than 75% (Fig. 3 and 4). The sedimentation of the blood cells during centrifugation does not inhibit the pumping action, as the air pressure is high enough to resuspend the cells during the inward pumping phase and transfer them over the entire radial distance of 40 mm into the collection chamber. The minimum duration of an inward pumping cycle depends on the liquid volume and its properties, in addition to the spin protocol. For a 200 µl sample, the compression period varies from 6 s for water to 14 s for the lysis buffer, while the collection period varies from 5 s for water at 30 Hz s^{-1} to 75 s for the lysis buffer at 1 Hz s^{-1}.

In order to save space for further fluidic modules upstream or downstream in the vicinity of the pumping module, the compression chamber was reduced from 549 µl to 255 µl for a further experiment: a 330 µl water sample was pumped radially inwards using three pump cycles. During the third pump cycle, the optional siphon that was employed in this experiment was primed because the fill level in the collection chamber exceeded the siphon crest. Consequently, the liquid in the collection chamber was drained off through the siphon and pumped again radially outwards. The overall pump efficiency of the three pump cycles was 91.3 $\pm$ 0.5% (simulation: 91.0%).

Conclusions

We developed a simple, fast and robust method to pump liquids radially inwards under continuous rotation. The method requires centrifugation only, which is intrinsically available on every centrifugal microfluidic platform. It does not require any other assistive equipment, displacer liquids or surface modification. CDIP can be applied to liquids and suspensions having wide ranges of density, viscosity or surface tension. Four liquids from typical biological applications have been successfully pumped inwards. The inward pumping over a radial distance of 40 mm in 11 s had a pump efficiency of more than 75%, which can be improved to more than 90% by having multiple pump cycles. The network simulation was employed to predict and optimize the pump performance. It can be used to quantitatively adapt the inward pumping module for integration into more complex centrifugal MF processes. CDIP enables using the entire radial path of a centrifugal platform multiple times with multiple fluidic channels. It thus paves the way to interconnect several functional building blocks, such as cell lysis,[17] DNA purification[10] and genotyping[18] to fully integrated sample-to-answer analysis systems.

References

1 R. Gorkin, J. Park, J. Siegrist, M. Amasia, B. S. Lee, J. M. Park, J. Kim, H. Kim, M. Madou and Y. K. Cho, *Lab Chip*, 2010, **10**, 1758–1773.
2 M. Madou, J. Zoval, G. Y. Jia, H. Kido, J. Kim and N. Kim, *Annu. Rev. Biomed. Eng.*, 2006, **8**, 601–628.
3 D. C. Duffy, H. L. Gillis, J. Lin, N. F. Sheppard and G. J. Kellogg, *Anal. Chem.*, 1999, **71**, 4669–4678.
4 S. Haeberle and R. Zengerle, *Lab Chip*, 2007, **7**, 1094–1110.
5 Z. Noroozi, H. Kido, M. Micic, H. Pan, C. Bartolome, M. Princevac, J. Zoval and M. Madou, *Rev. Sci. Instrum.*, 2009, **80**, 075102.
6 M. Amasia and M. Madou, *Bioanalysis*, 2010, **2**, 1701–1710.
7 S. Haeberle, T. Brenner, R. Zengerle and J. Ducrée, *Lab Chip*, 2006, **6**, 776–781.
8 M. Grumann, A. Geipel, L. Riegger, R. Zengerle and J. Ducrée, *Lab Chip*, 2005, **5**, 560–565.
9 Z. Noroozi, H. Kido, R. Peytavi, R. Nakajima-Sasaki, A. Jasinskas, M. Micic, P. L. Felgner and M. J. Madou, *Rev. Sci. Instrum.*, 2011, **82**, 064303.
10 Y. K. Cho, J. G. Lee, J. M. Park, B. S. Lee, Y. Lee and C. Ko, *Lab Chip*, 2007, **7**, 565–573.
11 J. Ducrée, S. Haeberle, S. Lutz, S. Pausch, F. von Stetten and R. Zengerle, *J. Micromech. Microeng.*, 2007, **17**, S103–S115.
12 R. A. Gorkin III, C. E. Nwankire, J. Gaughran, X. Zhang, G. G. Donohoe, M. Rook, R. O'Kennedy and J. Ducree, *Lab Chip*, 2012, **12**, 2894–2902.
13 D. Mark, P. Weber, S. Lutz, M. Focke, R. Zengerle and F. von Stetten, *Microfluid. Nanofluid.*, 2011, **10**, 1279–1288.
14 S. Lutz, P. Weber, M. Focke, B. Faltin, J. Hoffmann, C. Müller, D. Mark, G. Roth, P. Munday, N. Armes, O. Piepenburg, R. Zengerle and F. von Stetten, *Lab Chip*, 2010, **10**, 887–893.
15 D. Mark, F. von Stetten and R. Zengerle, *Lab Chip*, 2012, **12**, 2464–2468.
16 L. Wang, M. C. Kropinski and P. C. H. Li, *Lab Chip*, 2011, **11**, 2097–2108.
17 H. Kido, M. Micic, D. Smith, J. Zoval, J. Norton and M. Madou, *Colloids Surf., B*, 2007, **58**, 44–51.
18 M. Focke, F. Stumpf, G. Roth, R. Zengerle and F. von Stetten, *Lab Chip*, 2010, **10**, 3210–3212.
19 K. Abi-Samra, L. Clime, L. Kong, R. Gorkin III, T. H. Kim, Y. K. Cho and M. Madou, *Microfluid. Nanofluid.*, 2011, **11**, 643–652.
20 M. C. R. Kong and E. D. Salin, *Anal. Chem.*, 2010, **82**, 8039–8041.
21 A. Kazarine, M. C. R. Kong, E. J. Templeton and E. D. Salin, *Anal. Chem.*, 2012, **84**, 6939–6943.
22 M. C. R. Kong, A. P. Bouchard and E. D. Salin, *Micromachines*, 2012, **3**, 1–9.
23 C. Y. Li, X. L. Dong, J. H. Qin and B. C. Lin, *Anal. Chim. Acta*, 2009, **640**, 93–99.
24 R. Gorkin, L. Clime, M. Madou and H. Kido, *Microfluid. Nanofluid.*, 2010, **9**, 541–549.
25 H. Bruus, *Theoretical microfluidics*, Oxford University Press, 1, 2008.